Manipulation of the Radiation Characteristics of a Patch Antenna by Small Ferrite Disks Inserted in Its Cavity Domain

Michael Sigalov, Reuven Shavit, *Senior Member, IEEE*, Roman Joffe, and E. O. Kamenetskii

***Abstract*—In this paper, it is shown how the radiation characteristics of a patch antenna can be manipulated by a small number of normally magnetized ferrite disks inserted in the resonant region of the patch. It is shown that a one- and dual-band circular polarized microstrip antenna can be obtained by taking advantage of the interaction of the antenna cavity field with the magnetized ferrite disks. The scattering and radiation parameters of the antenna are investigated. The dependence of the axial ratio and the return loss of the antenna on the position and the number of ferrite disks underneath the patch are analyzed. Experimental and simulation results are in good agreement.**

***Index Terms*—Circular polarization, ferrite, microstrip antenna.**

I. Introduction

THE inherent anisotropy and nonreciprocal properties of ferrite materials make them very attractive for use in different types of antenna applications. The low-loss dielectric properties of ferrite materials allow the electromagnetic (EM) waves to penetrate into the ferrite and results in an effective interaction between the electromagnetic waves and the ferrite magnetization. The topic of patch antennas printed on ferrite substrate is well documented in the literature [1]–[15]. In [1]–[3], it is shown how variation of the external magnetic bias of the ferrite substrate on which patch antennas are printed can be used to control their operating frequency, and in [4]–[8], it is shown how it can control the beam steering of the radiation pattern and its radar cross section. In [9] and [10], it is described how high and magnetically tunable permeability of the ferrite substrate can be used to reduce the antenna dimensions. Several papers have also considered the possibility of creating magnetically switchable right and left circularly polarized patch antennas printed on a magnetized ferromagnetic substrate [11], [12] or using a ferrite post underneath the patch [13], [14]. In [15], the authors had shown that insertion of a small normally magnetized ferrite disk into the cavity region of a patch antenna leads to very specific topological-phase characteristics. It was demonstrated that the power flow lines of the microwave-cavity fields interacting with a ferrite sample, in the proximity of its ferromagnetic resonance (FMR), may form whirlpool-like EM vortices. In [16] and [17], it is shown that if a microwave resonator contains enclosed gyrotropic-medium samples, the electromagnetic-field eigen functions could be complex, and the EM fields in the resonance region under the patch antenna do not exhibit a standing wave behavior. Accordingly, the EM fields have a propagation wave behavior, and vortices of power flow are generated in the cavity region of the patch antenna [15].

In this work, it is proposed to use small particles of ferrite materials embedded into the cavity region of the patch antenna, instead of use of full ferrite substrate, to manipulate its radiation characteristics. This concept offers a more flexible design, simplicity, and significant cost reduction. Moreover, it is demonstrated numerically and experimentally that the far-field characteristics of the patch antenna can be manipulated by the ferrite disks embedded in the cavity region. In Section II, a brief description of the basic properties of the EM field propagation in ferrite materials is described, and the methods to manipulate the radiation characteristics of a patch antenna by small ferrite disk samples inserted in the cavity region of the antenna are discussed. It is shown that different types of radiating field polarizations can be obtained simultaneously in different frequency bands by appropriate manipulations of the number of ferrite disks, their magnetization properties, and their location under the patch. This is a new feature in patch antennas printed on a ferrite substrate as far as the author's knowledge. The radiation parameters of the antenna are investigated and a parametric study of the radiation characteristics for one and two ferrite disks in the cavity region of the antenna is conducted. In Section III simulation and experimental results are presented. All simulation results in this work have been obtained using HFSS commercial software based on the finite-element method (FEM). Two prototype antennas with one and two ferrite disks were built and tested. The agreement between the measured and simulation data is satisfactory. In the current study, a bulky external dc magnet was used for demonstrating the physical phenomena involved, but in future work, for miniaturization purposes, the intention is to use small permanent magnets under the ferrite particles or magnetized ferrite disks.

Manuscript received May 03, 2012; revised December 25, 2012; accepted January 17, 2013. Date of publication January 25, 2013; date of current version May 01, 2013.

The authors are with the Department of Electrical and Computer Engineering, Ben Gurion University of the Negev, Beer-Sheva 84105, Israel. (e-mail: sigalov@ee.bgu.ac.il; rshavit@ee.bgu.ac.il; ioffr1@gmail.com; kmntsk@ee.bgu.ac.il).

Color versions of one or more of the figures in this paper are available online at http://ieeexplore.ieee.org.

Digital Object Identifier 10.1109/TAP.2013.2242830

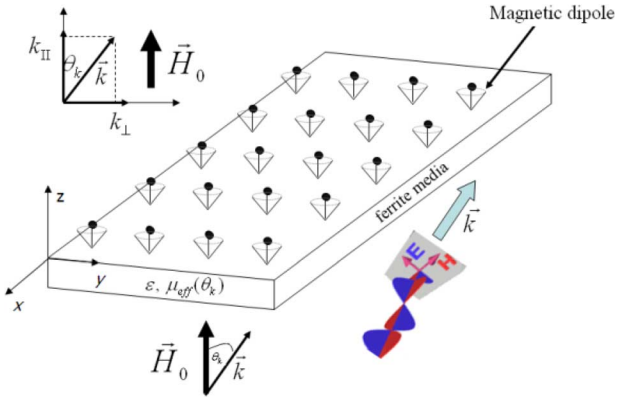

Fig. 1. Ferrite material illuminated by an electromagnetic wave.

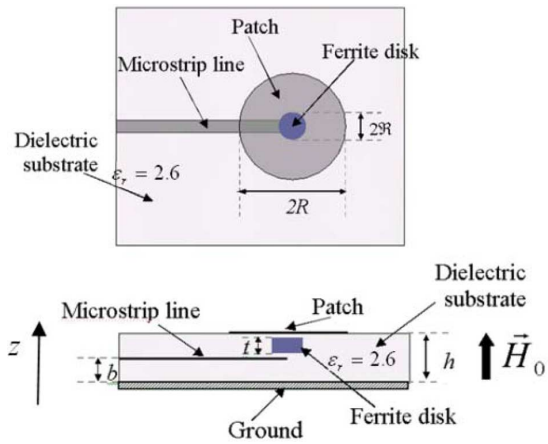

Fig. 2. Circular patch antenna with ferrite disk in the substrate region.

II. Theory

A. EM Field Propagation in a Ferrite Material

The propagation properties of an EM field in a ferrite material depend on the angle between the bias magnetic field and the direction of the propagation vector $\overrightarrow{k}$ of the EM field [16], [18]. Fig. 1 shows an infinite ferrite medium biased by an external field $\overrightarrow{H}_0$ and its precessing magnetic moments. The medium is illuminated by an EM plane wave with the propagating vector $\overrightarrow{k}$ at an angle θ_k with the direction of the dc bias magnetic field. The propagation constant k of the EM wave in the ferrite is dependent on the effective permeability [16]

$$\mu_{\text{eff}}(\theta_k) = \frac{2+\sin^2\theta_k(\mu_\perp-1)\pm\sqrt{\sin^4\theta_k(\mu_\perp-1)^2+4\cos^2\theta_k\frac{\mu_a^2}{\mu^2}}}{2\left(\sin^2\theta_k+\frac{\cos^2\theta_k}{\mu}\right)} \tag{1}$$

in which $\mu_\perp = (\mu^2-\mu_a^2)/(\mu)$. Here, μ is the diagonal term, and μ_a is the off-diagonal term in the permeability tensor $\overline{\overline{\mu}}$ [16]. Consider two limit cases of EM wave propagation vector, parallel and perpendicular to the internal dc magnetic field. In the case of EM wave propagation vector parallel to the direction of the internal magnetic field $\overrightarrow{H}_i(\theta_k = 0^\circ)$, the propagation mechanism of the EM wave in the ferrite medium can be best described by two circular polarized propagating waves with different propagation constants. The propagation constant for the right-hand circular polarization (RHCP) is $k_{\|}^{\text{RHCP}} = \omega\sqrt{\varepsilon\mu^{\text{RHCP}}}$ with $\mu^{\text{RHCP}} = \mu+\mu_a$, and for the left-hand circular polarization (LHCP) is $k_{\|}^{\text{LHCP}} = \omega\sqrt{\varepsilon\mu^{\text{LHCP}}}$ with $\mu^{\text{LHCP}} = \mu-\mu_a$.

The effective permeability values μ^{RHCP} and μ^{LHCP} are complex and vary with EM wave frequency or dc magnetic field. In the case of an EM wave propagating perpendicular to the direction of $\overrightarrow{H}_i$ ($\theta_k = 90^\circ$), the propagation mechanism of the EM wave in the ferrite medium can be best described by the so-called *ordinary and extraordinary propagation waves*. Accordingly, the propagation constant for the ordinary wave is $k = \omega\sqrt{\varepsilon\mu_0}$, and the propagation constant for the extraordinary wave is $k = \omega\sqrt{\varepsilon\mu_\perp}$.

B. Patch Antenna With Embedded Ferrite Disks

In this part, the proposed structure of the patch antenna with an embedded ferrite disk in the cavity region is considered. Fig. 2 shows the proposed antenna configuration with one ferrite disk, which consists of a circular patch with radius $R = 17$ mm, printed on a substrate with dielectric constant $\varepsilon_r = 2.6$, substrate thickness $h = 3.048$ mm and is fed by a dielectric loaded microstrip line with substrate thickness $b = 1.524$ mm through EM coupling.

The fields of the dominant TM_{110} mode under the patch, without the ferrite disk existence, can be approximated by the fields of an equivalent cylindrical resonator with magnetic walls with top and bottom conductive walls. The electric field of this mode can be expressed by [19]

$$\begin{aligned}\overrightarrow{e}_{\text{TM}_{110}}(r,\varphi,t) &= \hat{z}E_0J_1(kr)\cos(\varphi)\cos(\omega t)\\ &= \hat{z}\frac{E_0}{2}J_1(kr)[\cos(\omega t-\varphi)+\cos(\omega t+\varphi)]\end{aligned} \tag{2}$$

in which the distribution of the electric field along the radial coordinate is described by the first-order Bessel function $J_1(kr)$, and $\cos(\omega t-\phi)$ and $\cos(\omega t+\phi)$ represent two azimuthally right and left propagating waves in opposite directions. The superposition of these azimuthally running waves, with the same amplitude, results in a standing wave behavior of the electric field with linear polarization and resonant frequency at 3.08 GHz.

The ferrite disk with radius $\Re = 4$ mm and thickness $t = 1$ mm is inserted in the cavity region of the patch antenna. The material properties of the ferrite disk are $4\pi M_s = 1780$ Gauss, $\varepsilon_r = 15$, $\tan\delta = 2*10^{-4}$, $\Delta H = 30$ Oe.

Here, M_s is the saturation magnetization of a ferrite material and ΔH is the linewidth near the ferromagnetic resonance. The dimensions of the ferrite disk were selected to avoid the propagation of the magnetic-dipolar modes in its volume and neglect the variation (nonhomogeneity) of the internal bias magnetic field along the thickness of the disk. Accordingly, a ratio of 1:8 between the ferrite's disk thickness to its diameter was chosen.

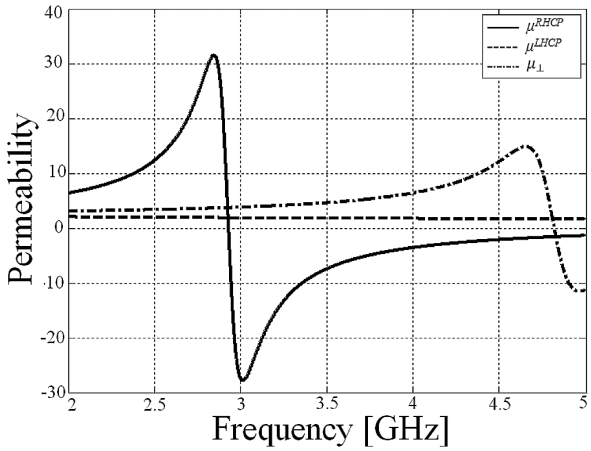

Fig. 3. Real parts of μ^{RHCP}, μ^{LHCP} and $\mu_\perp$ as a function of frequency.

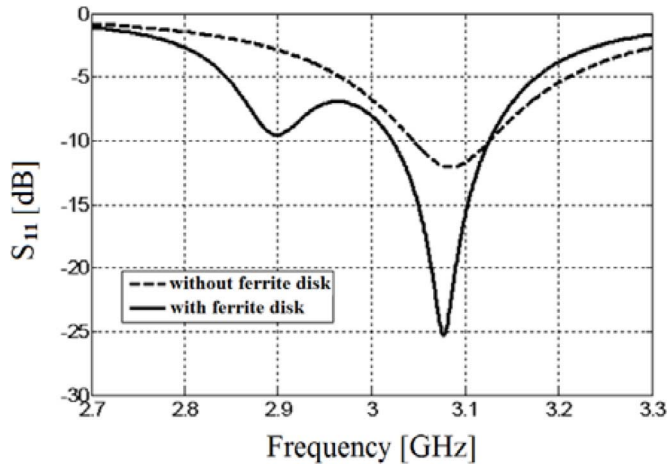

Fig. 4. Comparison between reflection coefficients, S_{11} of the patch antenna and the patch antenna with the embedded ferrite disk.

The ferrite disk is magnetized by an external dc magnetic field $H_0 = 2827$ Oe in the z-direction. In this case, the dc internal magnetic field is equal to $H_i = H_0 - 4\pi N_z M_s$, in which N_z is a coefficient depending on the disk geometry. For a thin cylindrical disk, $N_z = 1$ [18]. It is worth noting that, in this case, the internal dc magnetic field is nonhomogeneous along its radial line. Moreover, the dimensions of the ferrite disks were chosen much smaller than the dimensions of the patch antenna, such that this nonhomogeneity of the internal dc magnetic field has a negligible effect on the behavior of the patch antenna. The agreement between the experimental and simulation results confirms this assumption. Thus, the internal magnetic field is equal to $H_i = H_0 - 4\pi M_s = 1047$ Oe. The dependence of the real parts of μ^{RHCP}, μ^{LHCP} and $\mu_\perp$ on the frequency is shown in Fig. 3.

It is clear from Fig. 3 that μ^{RHCP} and $\mu_\perp$ have resonant behavior near the frequencies $f = 2.9$ GHz and $f = 4.7$ GHz, correspondingly. Fig. 4 shows the comparison between the reflection coefficients S_{11} of the patch antenna with and without the embedded ferrite disk. One can observe that the patch initial resonance splits in two separate resonances, one at $f_{01} = 2.88$ GHz and the other at $f_{02} = 3.08$ GHz. This fact can be attributed to a different coupling mechanism between the ferrite disk and the two azimuthally running waves in opposite directions in the cavity region.

Fig. 5 shows the reflection coefficient and axial ratio (AR) of the patch with the ferrite disk as a function of frequency for different disk radii.

One can observe that a split in the resonance frequency of the initial patch accompanied by two orthogonal circular polarizations is obtained for a ferrite radius of 4 and 5 mm, but for practical reasons, a ferrite disk with a 4-mm radius was chosen in this study. Moreover, close observation of the results presented in Fig. 3 shows that, at the patch resonant frequencies $f_{01} = 2.88$ GHz, $\mu^{\mathrm{RHCP}} > 0$, while for $f_{02} = 3.08$ GHz, $\mu^{\mathrm{RHCP}} < 0$. This implies that at the two resonant frequencies different coupling mechanisms apply.

In Fig. 6, the structure of the power flow vortices of the azimuthally left and right running fields at the two resonant frequencies due to the presence of the ferrite disk in the cavity region is presented.

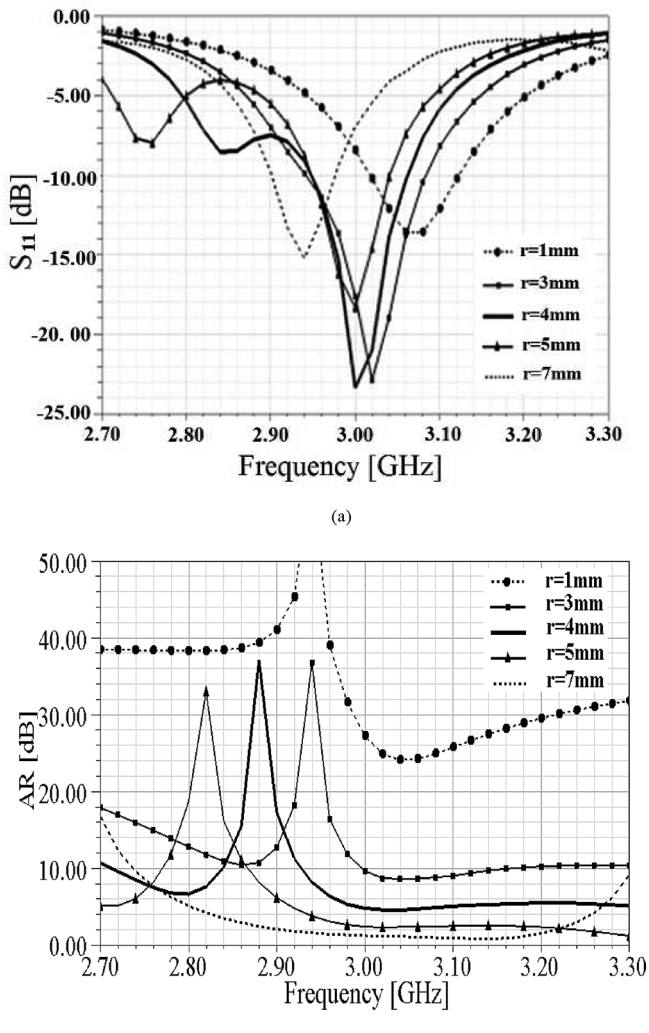

Fig. 5. Reflection coefficient of the antenna versus frequency with the ferrite disk radius as parameter: (a) reflection coefficient and (b) axial ratio.

One can observe that the EM fields under the patch at $f_{01} = 2.88$ GHz correspond to the wave running in the azimuthally

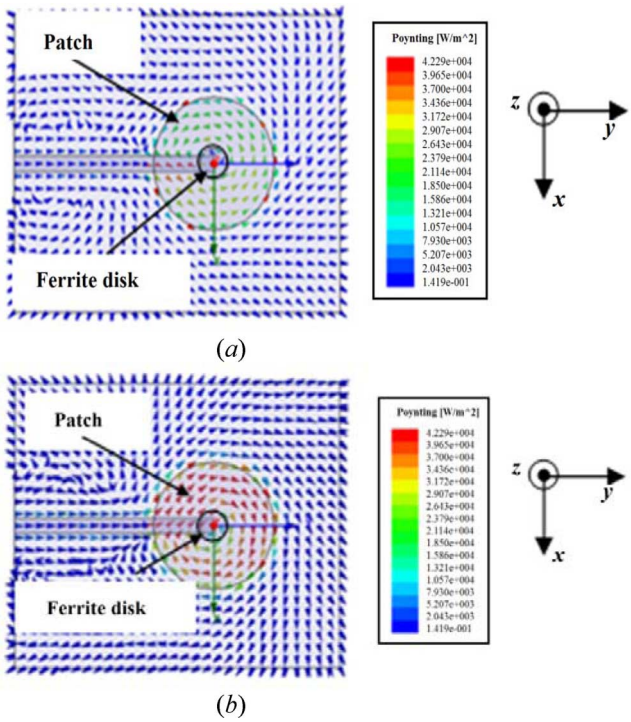

Fig. 6. Power flow vortices of the EM field in the cavity region of the patch: (a) $f_{01} = 2.88$ GHz and (b) $f_{02} = 3.08$ GHz.

left direction and at $f_{02} = 3.08$ GHz correspond to the wave running in the azimuthally right direction.

The implication of this observation to far-field radiation is that, at $f_{01} = 2.88$ GHz, the RHCP radiation is dominant, while at $f_{02} = 3.08$ GHz, the LHCP radiation is dominant. This observation is also supported by the simulation results of the AR in Fig. 5(b).

III. Numerical and Experimental Results

A. Single Band Circular Polarized Patch Antenna

The next step of our study was to optimize the reflection coefficient of the antenna and its performance with respect to LHCP at the resonant frequency of $f_{02} = 3.08$ GHz.

The reflection coefficient, the AR, and the antenna gain as a function of frequency with respect to the center location of the ferrite disk on the y-axis inside the resonator is shown in Fig. 7. One can observe from Fig. 7 that the best AR and gain are obtained for a ferrite disk center displacement of $y = -11$ mm. For this configuration, the axial ratio is about 1 dB [i.e., Fig. 7(b)], and the antenna gain is 7 dBic [i.e., Fig. 7(c)]. The reflection coefficient of the antenna is less than -15 dB [i.e., Fig. 7(a)]. The Copol (LHCP) and Xpol (RHCP) radiation patterns of the antenna at $f_{02} = 3.08$ GHz are shown in Fig. 8.

One can observe that the 3-dB beamwidth of the Copol is approximately 70°, and the Xpol level on the antenna axis is less than -25 dB. Fig. 9 shows the reflection coefficient and the AR with the ferrite disk radius as parameter. It actually shows that a ferrite disk with radius $\Re = 4$ mm is optimal in terms of

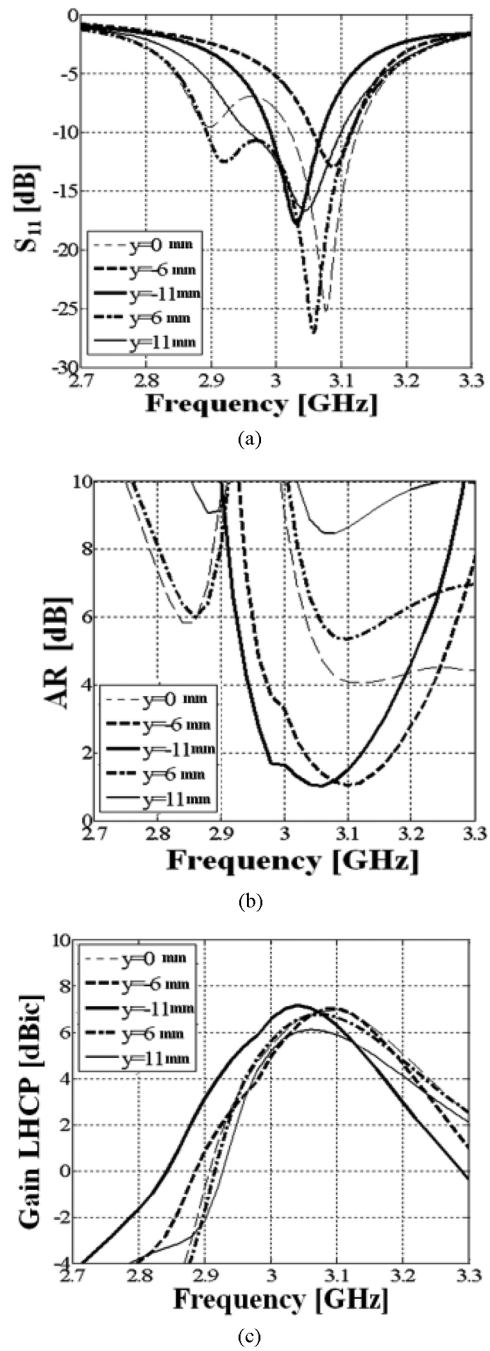

Fig. 7. Reflection coefficient, AR and LHCP gain of the antenna versus frequency with the ferrite disk center location as parameter: (a) reflection coefficient; (b) axial ratio; and (c) LHCP gain.

matching, and it exhibits minimal AR at the resonant frequency $f_{02} = 3.08$ GHz.

Further optimization of the patch characteristics can be obtained by insertion of an additional ferrite disk under the patch. Fig. 10 shows the geometry of the patch antenna with two disks separated apart by a distance $l = 22$ mm. Fig. 11 shows the variation effect of the second ferrite disk radius on the reflection coefficient and the AR. The saturation magnetization of the disks is identical and equal to 1780 Gauss and the bias magnetic field is 2827 Oe. One can observe that the optimum performance in terms of axial ratio is obtained for equal radii with

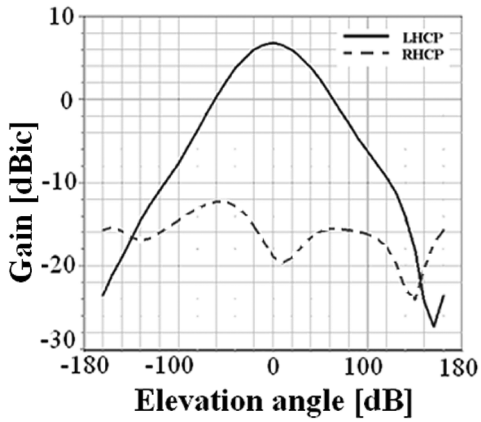

Fig. 8. Antenna radiation patterns (Copol-LHCP, Xpol-RHCP) at 3.08 GHz.

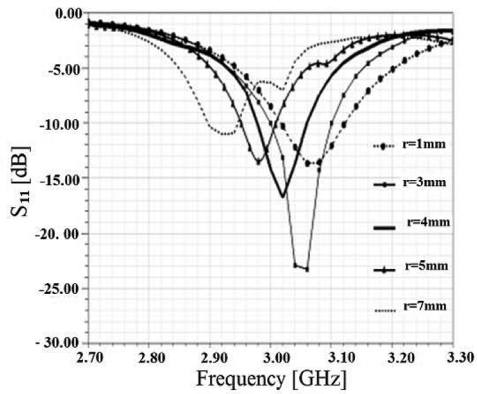

(a)

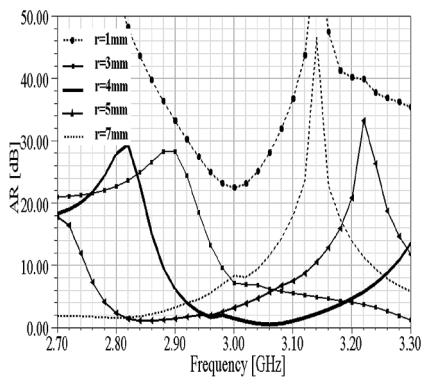

(b)

Fig. 9. Reflection coefficient and axial ratio of the antenna versus frequency with the ferrite disk radius as parameter: (a) reflection coefficient and (b) axial ratio.

$\Re = 4$ mm and is better than the comparable parameters obtained with a single disk displayed in Fig. 7. By symmetry, we can realize RHCP characteristics by reversing the direction of the bias magnetic field.

B. Dual-Band and Dual-Circular Polarization Patch Antenna

In this part of the paper, it will be shown that dual frequency band and dual-circular polarization can be achieved with the patch antenna. This feature can be obtained by insertion of two

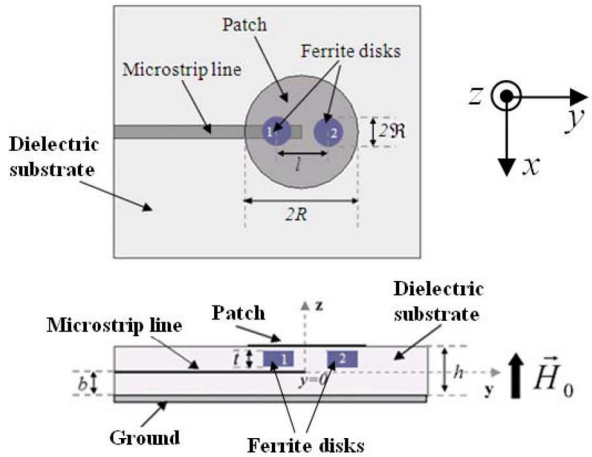

Fig. 10. Microstrip patch antenna with two ferrite disks.

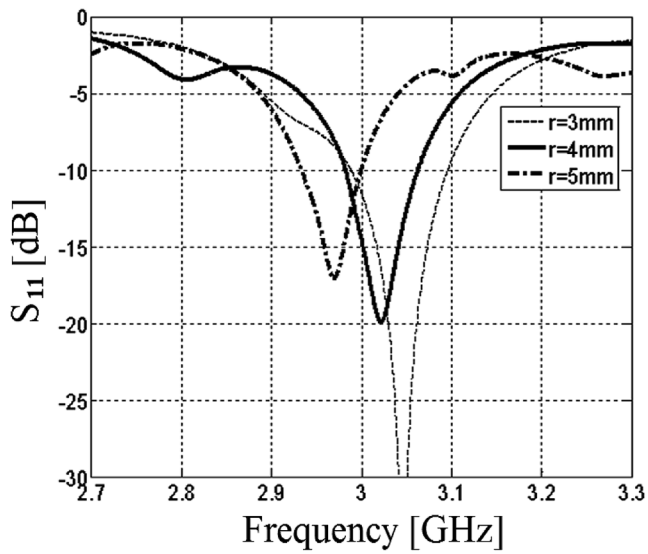

(a)

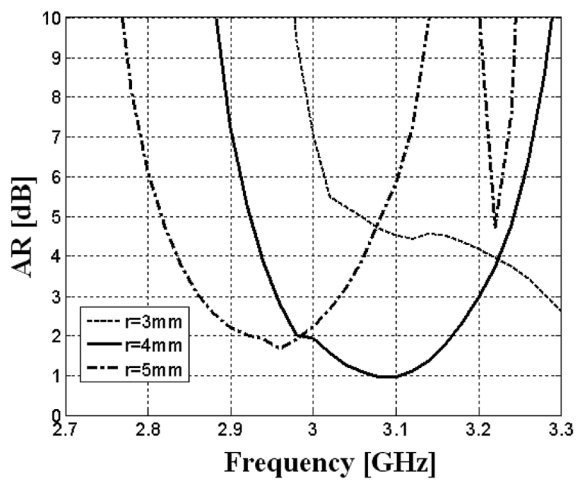

(b)

Fig. 11. Patch antenna with two ferrite disks and different radiuses of the second disk. (a) reflection coefficient and (b) axial ratio.

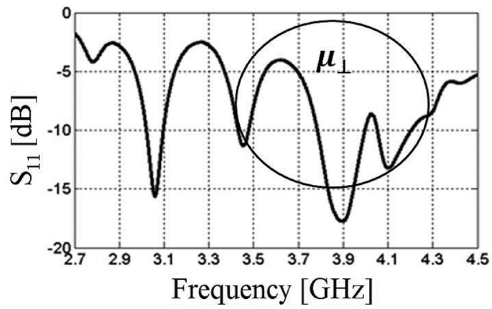

Fig. 12. Reflection coefficient of the patch antenna with two ferrite disks.

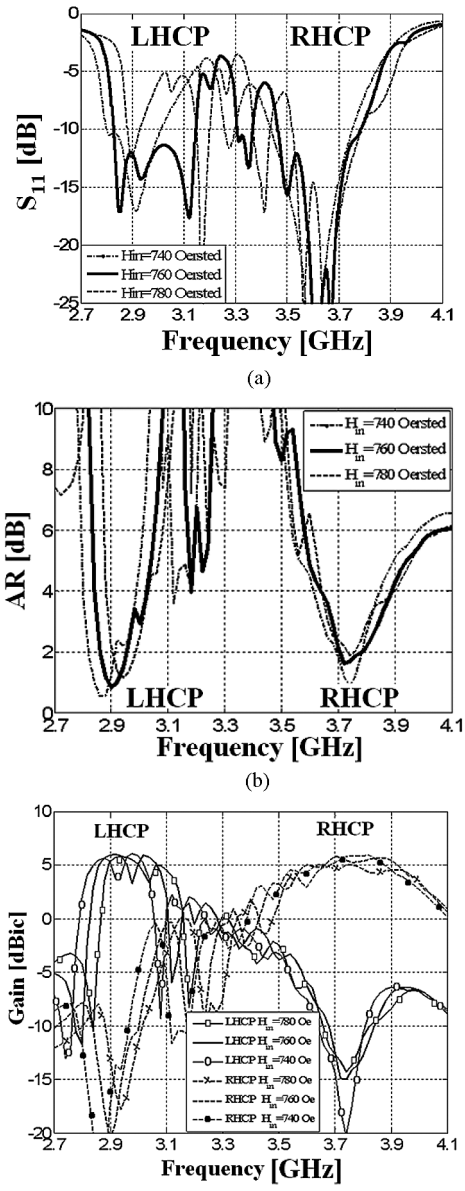

Fig. 13. Patch characteristics for different distances between the ferrite disks: (a) reflection coefficient; (b) axial ratio; and (c) gain.

or more ferrite disks in the cavity region of the antenna and appropriate optimization of the bias magnetic field.

Fig. 12 shows the reflection coefficient of the patch antenna with two ferrite disks with $\Re = 4$ mm separated 22 mm apart on the y-axis, as displayed in Fig. 10, but on an extended frequency scale. One can observe that additional resonance peaks appear in the frequency region, where the permeability $\boldsymbol{\mu}_\perp$ has a dominant

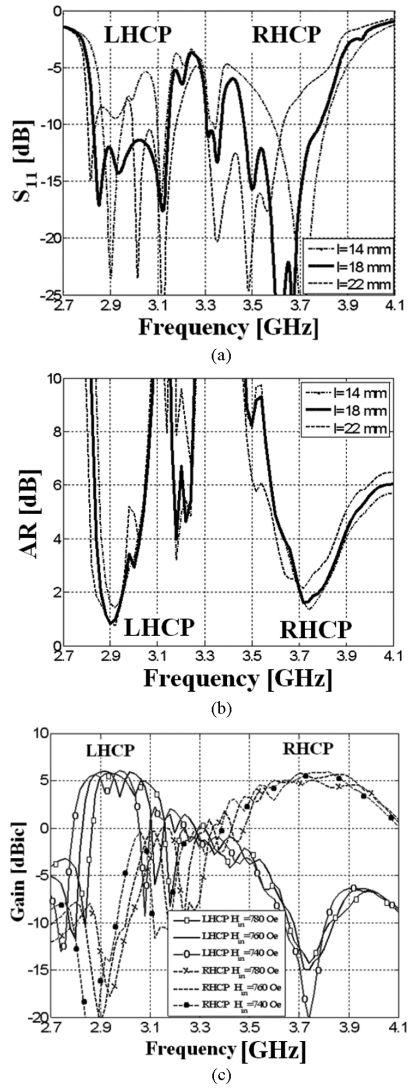

Fig. 14. Patch characteristics for different internal magnetic fields of the ferrite disks: (a) reflection coefficient; (b) axial ratio; and (c) gain.

resonance behavior (see Fig. 3) and strongly affect the behavior of the EM fields under the patch. These resonance peaks can be shifted down and coupled to the resonance of the patch at 3.08 GHz by variation of the internal magnetic field. Gradual reduction of the internal magnetic field from $H_{\rm i} = 1047$ Oe to $H_{\rm i} = 760$ Oe resulted in two frequency bands: one around 3 GHz, and the other around 3.7 GHz, as shown in Fig. 13. The polarization of the patch at 3 GHz is LHCP, while at 3.7 GHz is RHCP.

The optimal performance can be obtained by variation of the distance, l between the two disks under the patch and the internal magnetic fields of the disks. Fig. 13 shows the reflection coefficient, the AR, and the antenna gain (LHCP and RHCP) as a function of frequency for different distances between the disks in the cavity domain. One can observe that the optimum performance of the two frequency bands is obtained for $l = 18$ mm.

The optimum AR of the LHCP in the first frequency band around 2.9 GHz is 1 dB, while the AR of the RHCP in the second frequency band around 3.7 GHz is 1.5 dB. The maximum gain of the patch in both frequency bands is 5.5 dBic and shows a Xpol better than -20 dB. Fig. 14 shows the reflection coefficient, the

(*a*) (*b*)

Fig. 15. (a) Patch and ground plane. (b) Patch with one ferrite disk and feeding microstrip line.

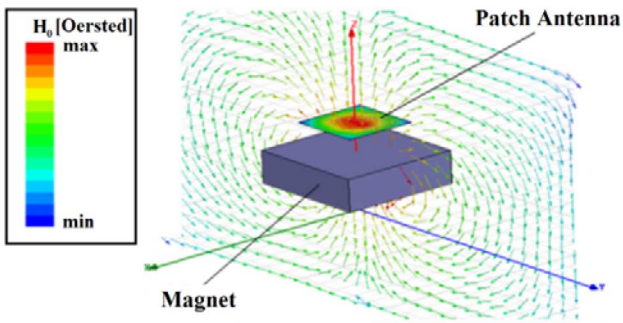

Fig. 16. Intensity of bias dc magnetic field.

AR, and the antenna gain (LHCP and RHCP) as a function of frequency for different internal magnetic fields.

One can observe that the optimum performance of the two frequency bands is obtained for internal magnetic field of $H_{\rm i} = 760$ Oe.

C. Experimental Results

For validation purposes, a prototype of the antenna with one ferrite disk (as shown in Fig. 2) was fabricated. The antenna and the feeding microstrip line were printed on ULTRALAM®2000 substrates of Rogers Corporation are shown in Fig. 15(a). The permittivity of the substrate is $\varepsilon_r = 2.6$, and its thickness is $b = 1.524$ mm. The ferrite disk used was made of yttrium iron garnet (YIG) from TCI Ceramics Company. The ferrite disk properties are as follows: $4\pi M_s = 1780$ Gauss, $\varepsilon_r = 15$, $\tan\delta = 2{*}10^{-4}$,, $\Delta H = 30$ Oe. The radius of the disk is $\Re = 4$ mm, and its thickness is $t = 1$ mm. The disk was placed at the position of $y = -11$ mm and magnetized by an external bias magnetic field of $H_0 = 2827$ Oe.

For magnetization of the ferrite disk, a permanent magnet with dimensions of 50 mm × 50 mm × 15 mm was placed at the bottom side of the patch antenna. In Fig. 16, one can observe the bias dc magnetic field distribution of the permanent magnet simulated by HFSS. The optimal intensity and distribution of the bias magnetic field for matching the simulation and measured data of S_{11}, AR, and gain was obtained at the distance of 13 mm from the permanent magnet surface.

Comparison between simulated and measured results for the patch antenna with one ferrite disk is shown in Fig. 17.

One can observe a satisfactory agreement between the measured and simulated results of the reflection coefficient S_{11}, AR, and the antenna gain. Fig. 18 shows a comparison between the simulated and measured results for the patch antenna with two ferrite disks placed at the distance $l = 18$ mm.

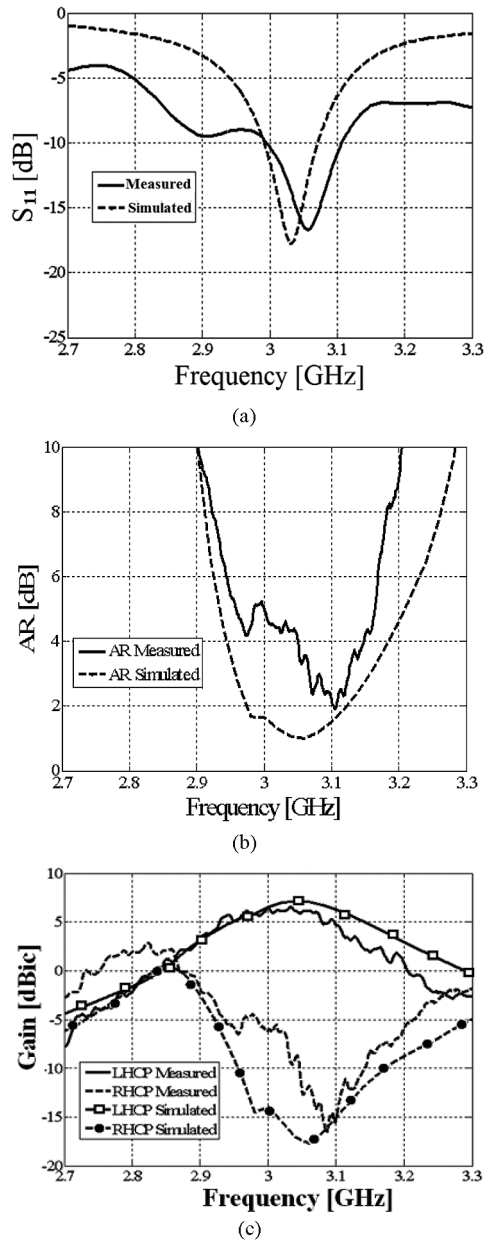

Fig. 17. Comparison of the simulated and measured results of the patch antenna with one ferrite disk: (a) Reflection coefficient; (b) axial ratio; and (c) LHCP and RHCP gains.

In the experiment, we encountered problems in the agreement between the simulated and measured data, mainly because of the nonhomogeneity in the bias field distribution of the dc magnet under the patch and the internal magnetic bias field distribution in the ferrite disks as described in [20] and [21]. The best agreement between the measured and simulation data as shown in Fig. 18 was obtained by changing the simulation parameters of the bias magnetic fields of the left and right ferrite disks under the patch (i.e., Fig. 14). The simulation result of the internal magnetic field of the left disk was $H_i = 760$ Oe and that of the right disk was $H_i = 820$ Oe.

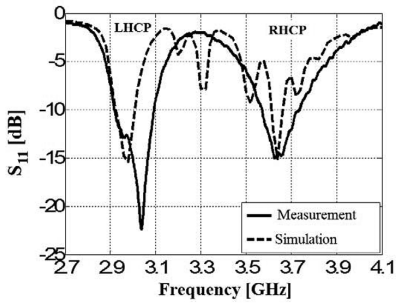

(a)

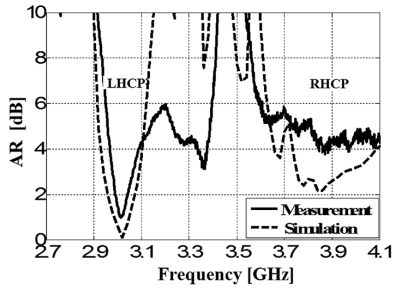

(b)

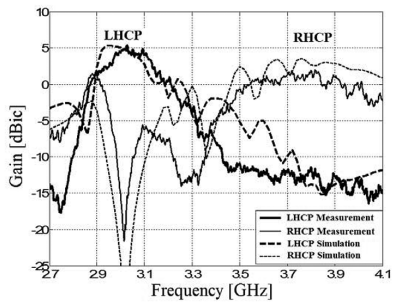

(c)

Fig. 18. Comparison of the simulated and measured results of the patch antenna with two ferrite disks: (a) reflection coefficient; (b) axial ratio; and (c) LHCP and RHCP gains.

IV. Summary

A new method to manipulate the radiation characteristics of the patch antenna by small normally magnetized ferrite disks inserted in the dielectric region under the patch is proposed. One- and dual-band circular polarized microstrip antennas were obtained by taking advantage of the interaction of the antenna cavity field with the magnetized ferrite disks. It was shown that an interaction of the electromagnetic fields within the cavity region of the patch and the magnetization of the ferrite disks is causing a rotating field, which yields circular polarization radiation. A continuous change in the radiating polarization from LHCP to RHCP through linear polarization is obtained with the frequency variation. The use of two ferrite disks in the antenna cavity region results in a dual-band and dual-circular polarization patch antenna. These types of antennas can find application in wireless communication systems to obtain better decoupling between the transmitter and receiver communication links of the system.

Acknowledgment

The authors would like to express their gratitude to M. Berezin for helping in performing the experiments through the course of this work.

References

[1] D. M. Pozar and V. Sanchez, "Magnetic tuning of a microstrip antenna on a ferrite substrate," *Electron. Lett.*, vol. 24, pp. 729–731, Jun. 1988.

[2] P. J. Rainville and F. J. Harackiewiz, "Magnetic tuning of a microstrip patch antenna fabricated on a ferrite film," *IEEE Microw. Guided Wave Lett.*, vol. 2, pp. 483–485, Dec. 1992.

[3] H. How and C. Vittoria, "Radiation frequencies of ferrite patch antennas," *Electron. Lett.*, vol. 28, no. 15, pp. 1405–1406, 1992.

[4] D. M. Pozar, "Radiation and scattering characteristics of microstrip antennas on normally biased ferrite substrates," *IEEE Trans. Antennas Propag.*, vol. 40, no. 9, pp. 1084–1092, Sep. 1992.

[5] A. Henderson and J. R. James, "Magnetized microstrip antenna with pattern control," *Electron. Lett.*, vol. 24, no. 1, pp. 45–47, 1988.

[6] A. D. Brown, J. L. Volakis, L. C. Kempel, and Y. Y. Botros, "Patch antennas on ferromagnetic substrates," *IEEE Trans. Antennas Propag.*, vol. 47, no. 1, pp. 26–32, Jan. 1999.

[7] B. Lee and F. J. Harackiewicz, "The RCS of a microstrip antenna on an in-plane biased ferrite substrate," *IEEE Trans. Antennas Propag.*, vol. 44, pp. 208–211, Feb. 1996.

[8] H. Y. Yang, J. A. Castaneda, and N. G. Alexopoulos, "The RCS of a microstrip patch on an arbitrarily biased ferrite substrate," *IEEE Trans. Antennas Propag.*, vol. 41, pp. 1610–1614, Dec. 1993.

[9] P. Ikonen, K. N. Rozanov, A. V. Osipov, and S. A. Tretyakov, "Magnetodielectric substrates in antenna miniaturization: Potential and limitations," *IEEE Trans. Antennas Propag.*, vol. 54, no. 11, pp. 3391–3399, Nov. 2006.

[10] K. Buell, H. Mosallaei, and K. Sarabandi, "A substrate for small patch antennas providing tunable miniaturization factors," *IEEE Trans. Microw. Theory Tech.*, vol. 54, no. 1, pp. 135–146, Jan. 2006.

[11] J. S. Roy, P. Vaudon, A. Reineix, F. Jecko, and B. Jecko, "Circularly polarized far fields of an axially magnetized circular ferrite microstrip antenna," *Microwave Opt. Tech. Lett.*, vol. 5, pp. 228–230, 1992.

[12] A. A. Mavridis and G. A. Kyriacou, "On the design of patch antennas tuned by transversely magnetized lossy ferrite including a novel resonating mode," *Progr. Electromagn, Res. (PIERS)*, vol. 62, pp. 165–192, 2006.

[13] A. A. Mavridis, G. A. Kyriacou, and J. N. Sahalos, "Analysis of circular patch antenna tuned by a ferrite post," *Microw. Opt. Tech. Lett.*, vol. 46, no. 3, pp. 234–237, 2005.

[14] A. A. Mavridis, G. A. Kyriacou, and J. N. Sahalos, "Printed antennas tuned by transversely magnetized ferrite operating at a novel resonant mode," *PIERS Online*, vol. 3, no. 8, pp. 1213–1216, 2007.

[15] M. Sigalov, E. O. Kamenetskii, and R. Shavit, "Chiral states of electromagnetic fields originated from ferrite-based electromagnetic vortices," *J. Appl. Phys.*, vol. 104, p. 113921, 2008.

[16] Gurevich and G. Melkov, *Magnetic Oscillations and Waves*. New York, NY, USA: CRC, 1996.

[17] E. O. Kamenetskii, M. Sigalov, and R. Shavit, "Microwave whirlpools in a rectangular-waveguide cavity with a thin-film ferrite disk," *Phys. Rev.*, vol. E 74, p. 036620, 2006.

[18] D. M. Pozar, *Microwave Engineering*, 3rd ed. New York, NY, USA: Wiley, 2005.

[19] C. A. Balanis, *Antenna Theory and Design*, 3rd ed. Mew York, NY, USA: Wiley, 2005.

[20] V. G. Kononov, C. A. Balanis, A. C. Polycarpou, and C. R. Birtcher, "Non-uniform field modeling of ferrite-loaded cavity-backed slot antennas," *IEEE Trans. Antennas Propag.*, vol. 57, no. 10, pp. 3402–3405, Oct. 2009.

[21] V. G. Kononov, C. A. Balanis, and C. R. Birtcher, "Analysis, simulation and measurements of CBS antennas loaded with non-uniformly biased ferrite material," *IEEE Trans. Antennas Propag.*, vol. 60, no. 4, pp. 1717–1726, Apr. 2012.

Michael Sigalov was born in Erevan, Armenia, on April 15, 1972. He received the B.Sc., M.Sc., and Ph.D. degrees in electrical and computer engineering from the Ben-Gurion University of the Negev, Beer-Sheva, Israel, in 2001, 2005 and 2009, respectively.

From 2009 to 2011, he worked as the Microwave Engineers Group Leader and later as the Head of the Applied Electromagnetic group in RF Dynamics, Ltd. (currently, Goji, Ltd.), where he was involved in the development of the microwave heating technologies and devices for the variety of industrial applications. Since the end of 2011, he has served as a CEO of Applied Electromagnetics, Ltd., Beer-Sheva, Israel, a company specializing in the development of microwave and antenna devices for the medical applications. His research interests are in areas of the localization and guiding of the microwave fields for antennas and other microwave applications, microwave devices for medical applications, microwave heating technologies, and devices for food processing applications.

Reuven Shavit (M'82–SM'90) was born in Romania on November 14, 1949. He received the B.Sc. and M.Sc. degrees in electrical engineering from the Technion—Israel Institute of Technology, Haifa, Israel, in 1971 and 1977, respectively, and the Ph.D. degree in electrical engineering from the University of California, Los Angeles, USA, in 1982.

From 1971 to 1993, he worked as a Staff Engineer and Antenna Group Leader in the Electronic Research Laboratories of the Israeli Ministry of Defense, Tel Aviv, Israel, where he was involved in the design of reflector, microstrip, and slot antenna arrays. He was also a part-time lecturer at Tel Aviv University, teaching various antenna and electromagnetic courses. From 1988 to 1990, he was associated with ESSCO, Concord, MA, USA, as a Principal Engineer involved in scattering analysis and tuning techniques of high-performance ground-based radomes. Currently, he is an Associate Professor with Ben-Gurion University of the Negev, Beer-Sheva, Israel, where he is doing research in microwave components and antennas. His present research interest is in the areas of smart antennas, tuning techniques for radomes, and numerical methods for design microstrip, slot, and reflector antennas.

Roman Joffe was born in U.S.S.R. (Latvia) on March 25, 1983. He received the B.Sc. degree in electrical and electronics engineering from Sami Shamoon College of Engineering (SCE), Beer-Sheva, Israel, in 2009 and the M.Sc. degree in electrical and computer engineering from Ben Gurion University of the Negev, Beer-Sheva, Israel, in 2012.

Since 2012, he has been working towards the Ph.D. degree in electrical and computer engineering from Ben Gurion University. His current research interests include microwave sensing and microwave microscopy of dielectric, magnetic and biological materials and structures, spectral properties of magnetostatic waves and oscillations and interaction of magnetostatic waves and oscillations with dielectric and chiral materials.

E. O. Kamenetskii, photograph and biography not available at the time of publication.